

# HIGH PRESSURE HYDROSTATIC THRUST BEARINGS IN MIXED LUBRICATION — EFFECTS OF ELASTIC DEFORMATION ON OPTIMUM CONDITIONS

**Toshiharu Kazama**

Dept. of Mechanical Systems Engineering, Muroran Institute of Technology, 27-1, Mizumoto-cho, Muroran, 050-8585, JAPAN  
kazama@mmm.muroran-it.ac.jp

**Mitsuru Fujiwara**

Dept. of Mechanical Systems Engineering, Muroran Institute of Technology

**Atsushi Yamaguchi**

Yokohama National University

**Abstract.** *The effects of elastic deformation on tribological characteristics and optimum conditions of circular hydrostatic thrust bearings for high pressure oil/water hydraulic pumps/motors are discussed experimentally and theoretically in mixed to fluid film lubrication. The test bearings with the diameter 20 mm were made of bearing steel, carbon steel and plastics, of which surface roughness was 0.05 to 3.6  $\mu\text{mRa}$ . The maximum supply pressure, maximum bearing load and the rotational speed were specified as 55 MPa, 15 kN and 2 rps respectively. The hydraulic oil with ISO VG 32 was supplied. The frictional torque and the leakage flow rate were measured; the power losses were evaluated. In parallel a mixed lubrication model, combining the asperity-contact mechanism proposed by Greenwood and Williamson and the average flow model by Patir and Cheng, adding the effects of adsorbed film and elastic deformation, was developed and solved numerically. In conclusion, as the supply pressure was higher, the elastic modulus was smaller and/or the surface roughness was smaller, the elastic effects became noticeable and the optimum conditions based on the minimum power loss changed. The theoretical solutions showed a good agreement with the experimental data.*

**Keywords.** *tribology, mixed lubrication, hydrostatic bearings, surface roughness, fluid power systems*

## 1. Introduction

Hydraulic pumps and motors are expected to work suitably under high pressure operating conditions. The reliability and efficiency of the equipment are conspicuously influenced by tribology of the bearing and seal parts (Yamaguchi, 1986). Some of the parts like a slipper (Shute and Turnbull, 1963; Iboshi and Yamaguchi, 1982; Hooke and Li, 1988) and a hydrostatic valve plate (Yamaguchi, 1987) in swash plate type axial piston pumps/motors behave as hydrostatic bearings.

Typical hydrostatic bearings are usually designed and used under the full film lubricating conditions since the primary advantage of the bearings is that a pair of two surfaces facing each other can be separated completely by fluids pressurized externally without relative motion of the surfaces. The basic theory (Fuller, 1984; Hamrock, 1994; Williams, 1994) and the design charts (Wilcock and Booser, 1957; JAST, 2001) of the hydrostatic bearings have been well established. However, the theory and the charts were focused mainly on the bearings of machine tools (O'Donoghue and Rowe, 1969; Rohs, 1970; Masuko and Nakahara, 1972; Inazaki and Aoyama, 1990) and all of them were limited to fluid film lubrication.

Hydraulic pumps/motors strongly demand less leakage and compactness, which enforces smaller clearance of the same order as the roughness height. The hydrostatic bearings for hydraulic equipment are not assumed any more to be operated in full film lubrication, owing to interference and contact of the roughness asperities, and thus they compelled to be worked in mixed lubrication. In addition, the load acting on the bearing/seal parts in the pumps/motors changes basically in proportion to the discharge pressures, in contrast to that the load in machine tools varies under the constant supply pressure. The conventional models and methods are, therefore, unable to apply directly to the design of the hydrostatic bearing/seal parts in hydraulic pumps/motors.

The authors have conducted research on the mixed lubrication characteristics of hydrostatic bearings theoretically (Kazama and Yamaguchi, 1993) and experimentally (Kazama and Yamaguchi, 1995). In the theoretical approach, a mixed lubrication model (Yamaguchi and Matsuoka, 1992) was applied to the analysis of hydrostatic thrust bearings. The mixed lubrication model was combined with the asperity-contact mechanism proposed by Greenwood and Williamson (1966) and the average flow model by Patir and Cheng (1978, 1979), which was further included the effects of breakdown of adsorbed films, cavitation around asperities and micro-elastohydrodynamic (EHD) contacts. In the experimental approach, a circular hydrostatic thrust bearing tester was built and the tribological aspect in a wide range of operating conditions was explored (Kazama and Yamaguchi, 1995). The friction, leakage flow rate and the power loss in mixed to fluid film lubrication were chiefly discussed. The experiment was accomplished successfully and the results were in good agreement with the theoretical calculation. In these papers (Kazama and Yamaguchi, 1993, 1995), additionally, the normalized parameters used frequently and known as the bearing number or the Sommerfeld number were re-examined, and accordingly a ratio indicating hydrostatic balance was proposed, which was defined by the ratio of the load to the maximum hydrostatic load-carrying capacity. The physical meaning of the ratio was checked carefully and the usefulness for expressing the feature of the hydrostatic bearings was shown.

The experimental conditions were, however, confined to the maximum supply pressure of 4.9 MPa and the maximum rotational speed of  $5.0 \text{ s}^{-1}$ , in order to avoid some complex phenomena like elastic deformation and heat generation, which were somewhat lower than the operating conditions of actual hydraulic systems. The operating pressure and power density of future hydraulic pumps/motors are expected to increase. Thus, there has been a need of efforts to investigate, in particular, at a higher pressure condition. Such operating conditions yield an enhancement of elastic deformation of the bearing parts.

As regards elastic analysis of hydrostatically supported bearings, in 1960's the pioneers began to struggle with the problem. Dowson and Taylor (1967) reported on the elastohydrostatic behavior of load-carrying human and animal joints, which consisted of a soft lining of an articular cartilage upon a relatively rigid backing of bone. In parallel, Castelli, et al. (1967) carried out the analytical and experimental investigation of a hydrostatic axisymmetric compliant-surface thrust bearing. The elastohydrostatic performance of soft materials evaluated under the low load-carrying state, however, would be different from that of metals used generally as a machine element. Prabhu and Ganesan (1983a, b) studied the behavior of capillary compensated annular recess conical hydrostatic bearings under tilting and rotating conditions. The pressure levels in these papers were still lower than those of hydraulic pumps/motors.

Another trend related to hydraulic systems is the usage of tap water as an alternative working fluid, from the viewpoint of environmental protection. Developments in water-hydraulic equipment (Yamaguchi, 1978) demand frequently the use of plastics in the lubricating parts, which may cause noticeable elastic deformation due to lower modulus of elasticity. On this point, Wang and Yamaguchi (2002a) reported the characteristics of a disk-type hydrostatic thrust bearing supporting concentric loads, using the bearings made up of a combination of plastics and stainless steel, and simulating the major bearing/seal parts of water hydraulic pumps/motors. Afterwards, they established the numerical analysis method based on a two-dimensional elastohydrostatic model, which was extended to adapt it for a non-axisymmetric load acting on the thrust bearing and discussed theoretically the eccentric loading conditions (Wang and Yamaguchi, 2002b). The liquid tested was tap-water, whereas the conditions dealt in their study were limited to full film lubrication and the supply pressure up to 9 MPa.

In this study the elastic effects of the hydrostatic bearings are appraised in mixed to fluid film lubrication. A circular hydrostatic thrust bearing rig is built, and the experiment is conducted at the maximum supply pressure of 55 MPa and the approximate maximum load of 15 kN. In parallel, a lubrication model including the influence of surface deformation and asperity contact is developed, and then theoretical calculations are performed under the experimental conditions. Subsequently, comparing the experimental and theoretical results in a wide range of operating conditions, the physical phenomena in the bearing clearance at high pressure are revealed and the effects of elastic deformation on the optimum conditions are discussed.

The deformed shape of the bearing clearances would be categorized in two modes; concave and convex film profiles. The effects of the convex profiles due mainly to deformation of the hydrostatic pad have partially been reported theoretically (Kazama and Yamaguchi, 1995) and experimentally (Kazama, et al., 1998), and hence the effects of the concave profiles are discussed in this paper.

## 2. Experimental apparatus and procedure

### 2.1. High pressure hydrostatic bearing tester

Figure (1) shows the schematic diagrams of the experimental apparatus (Kazama, et al., 1996) which enabled to simulate a circular hydrostatic thrust bearing in mixed to fluid film lubrication. The test bearings consisted of two cylindrical specimens, which were installed so that these flat end-surfaces were contacted. The upper specimen whose outer radius was  $R_2$  had a hollow core which corresponded to a hydrostatic recess with the radial ratio  $a$  of the inner to outer radii being 0.5. The lower specimen was a solid cylinder. Table (1) lists the representative dimensions of the apparatus and conditions of the experiment.

The upper specimen was made of carbon steel with standard heat treatment, designated as S45C (0.42~0.48%C) in the Japanese Industrial Standards, JIS, and the surface of the sealing land was finished with two grades of roughness: approximately, 0.5 and  $3.6 \mu\text{mRa}$ . The lower specimens were made of chromium-molybdenum bearing steel hardness designated as SUJ2 (0.95~1.10%C, 1.30~1.60%Cr) in JIS (elastic modulus  $E=206 \text{ GPa}$ ; Poisson ratio  $\nu=0.3$ , for reference) and plastics of polyetheretherketone as PEEK ( $E=3.3 \text{ GPa}$ ;  $\nu=0.21$ , for reference). The waviness of the specimens was removed by lapping before a specific roughness was treated. The Shore hardness  $H_s$  of the upper and lower metallic specimens was  $H_s=31\sim40$  and  $H_s>80$  respectively. For the sake of convenient, the upper specimens of the test bearings were distinguished by the roughness grades: 'smooth' and 'rough'; the lower ones were discriminated by the materials: 'SUJ2' and 'PEEK'. The reason why the plastic specimens were used in this experiment was that the effects of the elastic deformation were examined clearly. Table (2) gives the materials and surface roughness of the upper and lower specimens of the test bearings.

Mineral oil based hydraulic fluid (ISO VG 32; viscosity  $\mu=27.2 \text{ mPa}\cdot\text{s}$ , density  $\rho=850 \text{ kg/m}^3$  at 313 K) was used as the test oil. In order to remove the contaminants in the oil as much as possible, hydraulic filters with the nominal filtration-particle-size of  $3 \mu\text{m}$  were installed in both on- and off-lines. A hydraulic cooler was used so as to suppress a rise in the oil temperature. The cooler installed in the return circuit connecting to the relief valves since no manufactured cooler, to stand such extra-high pressure, was available. The temperature of the supply oil, therefore,

could not be controlled precisely. The temperature of the leaked oil was measured by thermistors of which reading precision was 0.1 °C, and then the viscosity  $\mu$  and the density  $\rho$  were compensated for the input data of the calculation.

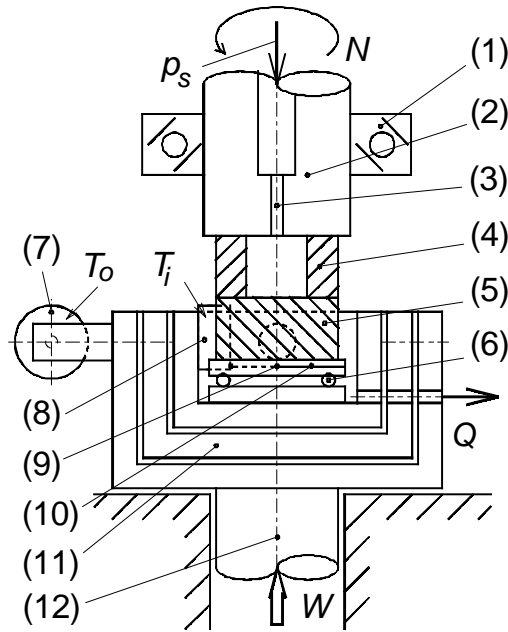


Figure 1. Schematic diagrams of circular hydrostatic thrust bearing tester (1. Rolling element bearings; 2. Driving shaft; 3. Restrictor; 4. Upper specimen (Test bearing); 5. Lower specimen (Test bearing); 6. Rolling element bearings; 7. Load cell; 8. Load cell; 9. Mount; 10. Wire; 11. Gimbals; 12. Hydraulic cylinder).

Table 1. Representative dimensions and experimental conditions.

Rotational speed	$N$	2	$s^{-1}$
Maximum supply pressure	$p_{s, \max}$	55	MPa
Outer bearing radius	$R_2$	10.0	mm
Maximum load, approximated	$W_{\max}$	15	kN

Table 2. Combination of test bearings in terms of materials and surface roughness  $\sigma$ .

upper / lower	$\sigma_2 / \sigma_1$ [ $\mu\text{m}/\mu\text{m}$ ]	Remarks
S45C / SUJ2	0.54 / 0.056	smooth
S45C / SUJ2	3.59 / 0.053	rough
S45C / PEEK	0.55 / 0.94	smooth
S45C / PEEK	3.61 / 0.62	rough

## 2.2. Experimental procedure

The pressurized test fluid was supplied at a constant pressure  $p_s$  by a hydraulic piston pump into the hydrostatic recess of the test bearing through a restrictor with the length  $l_c$  of 30 mm and the radius  $r_c$  of 1.0 mm. The upper specimen was rotated at a constant rotational speed  $N$  by an electric motor (7.5 kW). To avoid the tilt of the gap between the upper and lower specimens, the lower specimen was mounted on gimbals attached to a ram of a hydraulic cylinder. The static load  $W$  was acted by the hydraulic cylinder.

At the same time that the load  $W$  was varied from low to high to be operated in fluid film to mixed lubrication regimes, *vice versa*, the frictional torque  $T$  acting on the lower specimen and the volumetric flow rate  $Q$  leaked from the gap between the upper and lower specimens of the test bearings were determined. The torque  $T$  was measured by load-cell sensors. The flow rate  $Q$  was measured by two ways: When  $Q$  was larger, the volume in a period was measured using several sizes of measuring cylinders, and  $Q$  was determined. When  $Q$  was smaller, the mass in a period was measured, where the small pieces of industrial wipers were prepared beforehand; the oil leaked from the gap was absorbed into the wipers in a period; the mass of the wipers was weighed using a precision balance, and finally the mass

flow rate obtained by the difference in the mass was converted into  $Q$  by the oil density at the test temperature (Kazama and Yamaguchi, 1995).

### 2.3. Data arrangement

The experimental data are arranged by the following parameters. For describing the operating conditions, a ratio  $\zeta$  of the hydrostatic balance, corresponding to the normalized load, defined by (Kazama and Yamaguchi, 1993, 1995):

$$\zeta = \frac{W}{\pi(1-a^2)p_s R_2^2 / (-2 \log a)} \quad (1)$$

is introduced, where  $a$  is the ratio of the recess radius to the outer radius  $R_2$  of the test bearing,  $p_s$  is the supply pressure, and  $W (>0)$  is the load. The denominator in Eq. (1) means the maximum hydrostatic load-carrying capacity of concentrically loaded circular pad thrust bearings with rigid bodies in the steady state. The conditions of  $\zeta < 1$  and  $\zeta > 1$ , for the rigid bearings, imply the operation in fluid film and mixed lubrication respectively. The parameter  $\zeta$  can be enhanced and utilized to represent the operating conditions of the hydrostatic thrust bearings with elastic bodies.

Using the mean radius  $R$  of the bearing, the equivalent frictional coefficient  $f$  is defined by ( $T$ : frictional torque):

$$f = T / (RW) \quad (2)$$

The power loss  $L$  is given by the summation of the power losses due to leakage flow rate  $L_Q$  and those due to frictional torque  $L_T$ , namely;

$$L = L_Q + L_T = p_s Q + 2 \pi N T \quad (3)$$

where  $N$  is the rotational speed and  $Q$  is the leakage flow rate. For designing hydraulic pumps/motors, higher efficiency is essentially expected. Hence, the power loss  $L$  is selected as an objective/evaluation function in this paper and the loss  $L$  to be minimized should primarily be achieved.

## 3. Experimental results and discussion

### 3.1. Experiment of 'SUJ2' specimens

Figures (2) and (3) exhibit the effects of the surface roughness and the supply pressure  $p_s$  on the equivalent frictional coefficient  $f$  and the leakage flow rate  $Q$  respectively. The upper specimen was alternatively 'smooth' or 'rough' and the lower specimen was 'SUJ2'. For the rough specimen, the coefficient  $f$  increased at the hydrostatic balance ratio  $\zeta \approx 1$ , which was independent of the pressure  $p_s$  specified from 14 to 55 MPa. Meanwhile, for the smooth specimen, as  $p_s$  increased, the value of  $\zeta$  at a steep rise in  $f$  became larger and shifted to the right in Fig. (2). At  $p_s = 55$  MPa, the value of  $\zeta$  reached 1.5. It is noted that the frictional torque with the smooth specimen abruptly and sharply rose in the region of larger  $\zeta$ , so that the experiment was interrupted for safety.

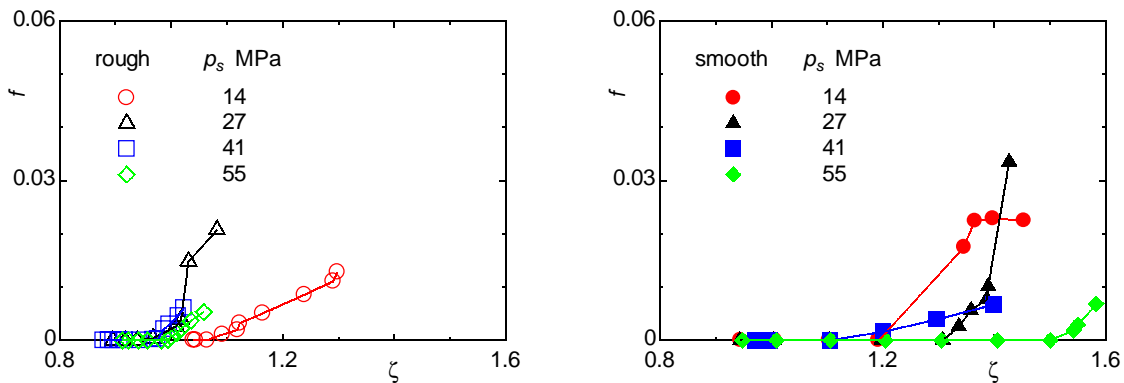


Figure 2. Effect of surface roughness on equivalent frictional coefficient  $f$  versus hydrostatic balance ratio  $\zeta$  in terms of supply pressure  $p_s$  (Experiment, SUJ2, Rough/Smooth).

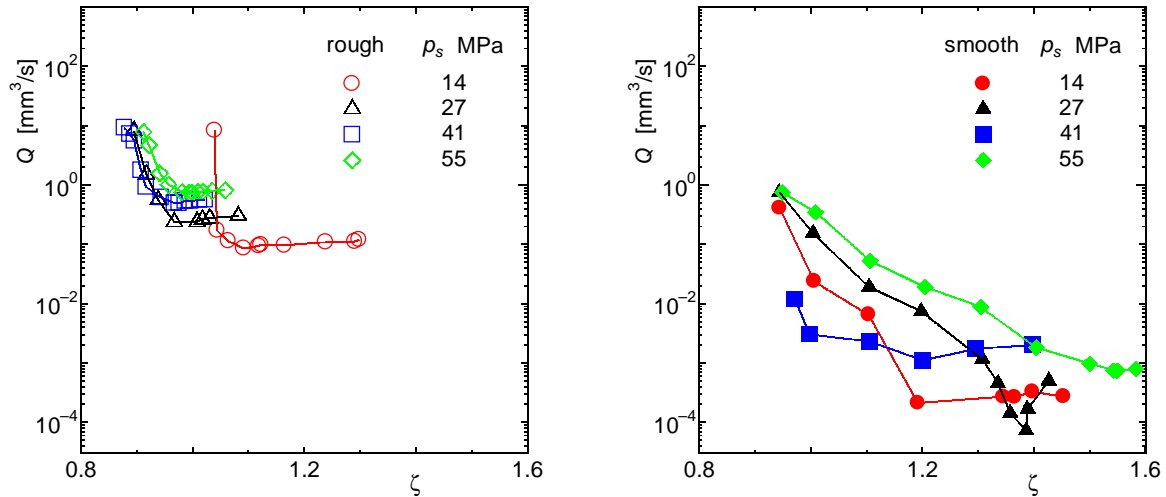


Figure 3. Effect of surface roughness on leakage flow rate  $Q$  versus hydrostatic balance ratio  $\zeta$  in terms of supply pressure  $p_s$  (Experiment, SUJ2, Rough/Smooth).

Comparing the flow rate  $Q$  between two roughness grades in Fig. (3),  $Q$  with the rough surface was larger than  $Q$  with the smooth surface. In addition,  $Q$  of 'rough' fell markedly at  $\zeta \approx 1$  and almost kept constant in the region of  $\zeta > 1$ . The tendency was independent of the supply pressure  $p_s$ , which coincided with the previous results under the lower  $p_s$  conditions (Kazama and Yamaguchi, 1995a).

Figures (4) and (5) depict the power losses  $L$  of 'SUJ2' specimens with the 'rough' and 'smooth' surfaces, corresponding to Figs. (2) and (3), respectively. In Fig. (4), for the rough specimens, the minimum power loss  $L_{min}$  was given at the condition of  $\zeta \approx 1$ . As the supply pressure  $p_s$  increased, the minimum  $L_{min}$  increased. At the same time, the gradient of  $L$  close to the ratio  $\zeta(L_{min})$  became large, which was mainly caused by an increase in the power loss due to frictional torque (Kazama and Yamaguchi, 1995). On the other hand, in Fig. (5), for the smooth specimens, the minimum  $L_{min}$  yielded visibly in  $\zeta > 1$ . As  $p_s$  increased, the region of  $\zeta$  where the curve of  $L$  in the vicinity of  $\zeta(L_{min})$  flattened widened.

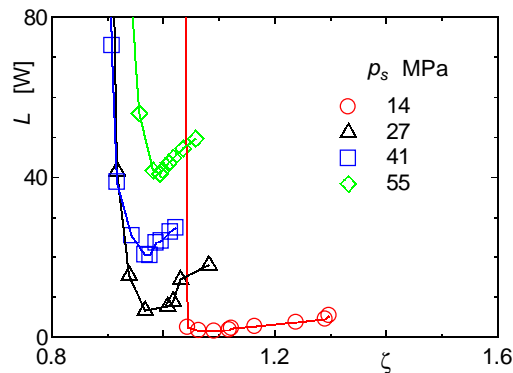


Figure 4. Effect of supply pressure  $p_s$  on power loss  $L$  versus hydrostatic balance ratio  $\zeta$  (Experiment, SUJ2, Rough).

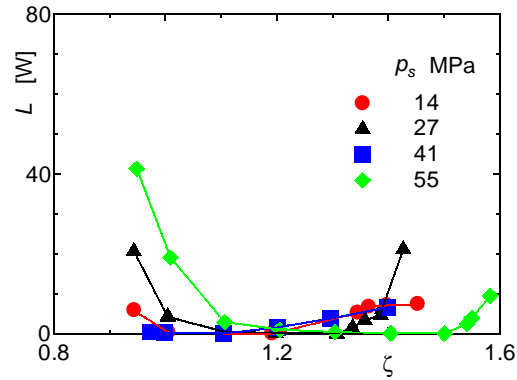


Figure 5. Effect of supply pressure  $p_s$  on power loss  $L$  versus hydrostatic balance ratio  $\zeta$  (Experiment, SUJ2, Smooth).

### 3.2. Experiment of 'PEEK' specimens

Figure (6) demonstrates the experimental data using the 'PEEK' specimens with the 'smooth' surface. Under the conditions of the higher supply pressure  $p_s$  and in the region of the larger balance ratio  $\zeta$ , for safety, the experiment was not conducted because the frictional torque suddenly increased and the bearing surface severely wore. We should mention here that the differences in the absolute values of the frictional coefficients and the power losses were not discussed because the boundary lubrication characteristics of 'PEEK' and 'SUJ2' were quite different and the comparison in terms of the absolute values was meaningless.

Comparing the aspects shown in Fig. (6) of 'PEEK' with Figs. (4) and (5) of 'SUJ2', one can see that, for the PEEK specimens, the influence of the supply pressure  $p_s$  on the power loss  $L$  was noticeable even in the lower pressure condition ( $p_s \leq 21$  MPa). In particular, the value of  $\zeta$  where  $L$  minimized apparently became larger than unity. At  $p_s=21$  MPa, the ratio  $\zeta(L_{min})$  reached 1.7. From the results by use of the material with a lower elastic modulus, *i.e.*, PEEK, and/or under the operating conditions at high pressure, it would be predictable that these results might be affected by the elastic deformation of the bearing surface. The prediction will be discussed in the next chapter based on the theoretical calculation.

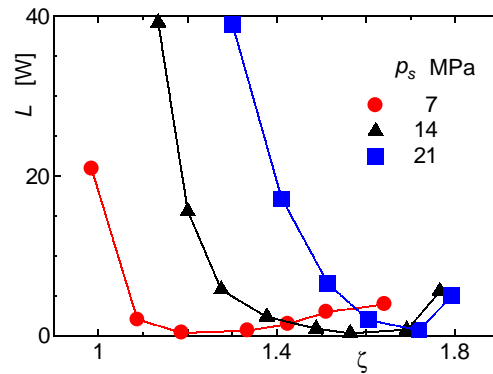


Figure 6. Effect of supply pressure  $p_s$  on power loss  $L$  versus hydrostatic balance ratio  $\zeta$  (Experiment, PEEK, Smooth).

## 4. Theoretical approach and comparison with experimental data

### 4.1. Numerical calculations

Theoretical analysis including asperity contact and elastic deformation is performed. The mixed lubrication model and the basic equations are described in the previous papers (Kazama and Yamaguchi, 1993; 1995b), except mainly for the equations of elasticity. The reader may refer to these papers for the details. The formulation for infinite elastic bodies can be found in other papers (Christensen, 1970; Kazama and Yamaguchi, 1997). The determination of the discharge coefficient of the nozzle is followed by the empirical expression (Hibi, et al., 1971). In the following calculation the assumptions of no heat generation, *i.e.*, isothermal/isoviscous conditions, concentric loads and the steady state are made. The input data are basically specified by the experimental conditions.

Figures (7) and (8) illustrate the clearance  $h/H$  profile, where  $H$  is a reference clearance and put  $H=\sigma$ , and the pressure distributions due to asperity  $p_a/p_s$  and fluid  $p_f/p_s$ , respectively. The surface corresponding to the lower specimen of the test bearings is assumed to be an infinite elastic body made of bearing steel hardness (SUJ2). As the supply pressure  $p_s$  increases, the surface of the bearing deforms like a concave shape as shown in Fig. (7). Such deformation results in a rise of  $p_f/p_s$  as given in Fig. (8), which brings about an increase in the hydrostatic load-carrying capacity. Under the condition of  $p_s=55$  MPa, the clearance  $h/H$  becomes smallest at the outer edge ( $r/R_2=1$ ). Under the condition of  $p_s=14$  MPa, the clearance  $h/H$  minimizes and the pressure  $p_a/p_s$  maximizes within the bearing-land. For the rigid condition, the profile of  $h/H$  keeps flat and the distribution of  $p_a/p_s$  remains constant, which are independent of  $p_s$ .

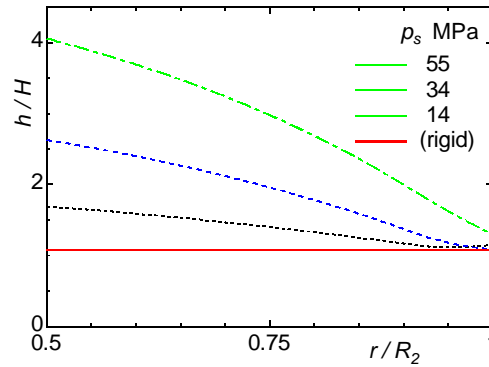


Figure 7. Calculated results of clearance  $h/H$  profiles of the land in terms of supply pressure  $p_s$  (SUJ2, Smooth,  $\zeta=1.5$ ).

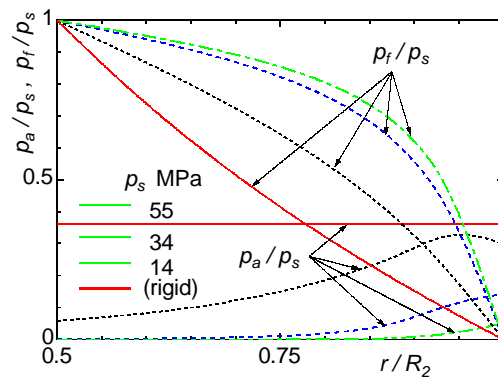


Figure 8. Calculated results of pressure distributions due to asperity-contact  $p_a/p_s$  and fluid  $p_f/p_s$  in terms of supply pressure  $p_s$  (SUJ2, Smooth,  $\zeta=1.5$ ).

#### 4.2. Influence of elasticity of bearing-parts

Figure (9) provides the comparison of the power losses  $L$  on the two assumptions of the elastic and rigid bodies. In the case of the rigid body, as the authors stated before (Kazama and Yamaguchi, 1993, 1995a), the power loss changes sharply and minimizes at the condition of the balance ratio  $\zeta \approx 1$ . The mechanism is recalled here that the loss  $L$  in  $\zeta < 1$ , corresponding to the fluid film lubrication regime, is involved mainly by the leakage and  $L$  in  $\zeta > 1$ , corresponding to the mixed lubrication regime, is by the friction, so that  $L$  minimizes at  $\zeta \approx 1$ . However, when the bearings consist of elastic bodies, the parts deform as a concave shape. As the supply pressure  $p_s$  increases, the power loss  $L$  changes gently and the value of  $\zeta$  at which  $L$  minimizes becomes larger than unity. In this case, the condition of  $\zeta(L_{\min})$  is given at  $\zeta(L_{\min}) \approx 1.3$  for  $p_s=55$  MPa. Of interest is that the aspect of the changes in  $L$  versus  $\zeta$  and the tendency of the effects of  $p_s$  on  $L$  in Fig. (9), based on the calculation, are similar with those in Figs. (5) and (6), obtained from the experiment.

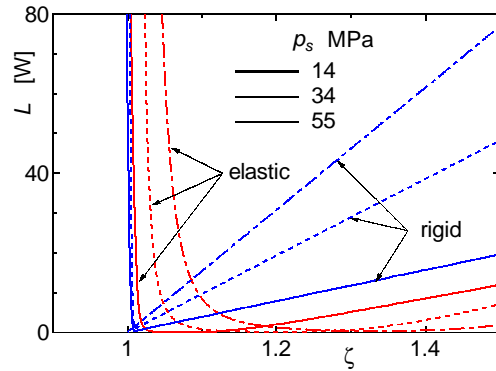


Figure 9. Influence of elasticity of bearing-parts on power losses  $L$  (Theory, SUJ2, Smooth).

### 4.3. Comparison between experimental and theoretical results

In Figures (10) through (12) the power loss  $L$ , leakage flow rate  $Q$  and the frictional coefficient  $f$  obtained from the experimental and theoretical approaches are compared. In Figure (10) the ratio  $\zeta$  ( $L_{\min}$ ) at the minimum power loss shifted to the right with increasing the supply pressure  $p_s$ . In Figures (11) and (12), as the pressure  $p_s$  increased, the leakage  $Q$  increased and the ratio  $\zeta$  at a sharp increase in the coefficient  $f$  became larger. Concerning the changes in  $L$  versus  $\zeta$  and the influence of  $p_s$  on  $L$ ,  $Q$  and  $f$ , the calculated results showed relatively good agreement with the experimental data.

From these results, one can conclude that the effect of elastic deformation is indispensable for the design of oil-hydraulic pumps/motors operating at high-pressure as well as for the development of tap-water hydraulic pumps/motors using plastic parts. From the viewpoint of the minimization of the power loss, the optimum ratio  $\zeta$  of the hydrostatic balance is given by a value being greater than unity. In other words, the idea may have the advantage of a reduction in size. However, the design concept utilized such elastic deformation would not be directly recommended, since the locally higher solid-contact pressure yields in mixed lubrication, which could cause wear and seizure.

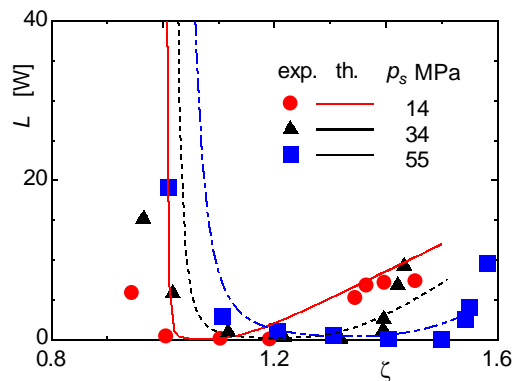


Figure 10. Comparison of power loss  $L$  between experiment and theory in consideration of elastic deformation (SUJ2, Smooth).



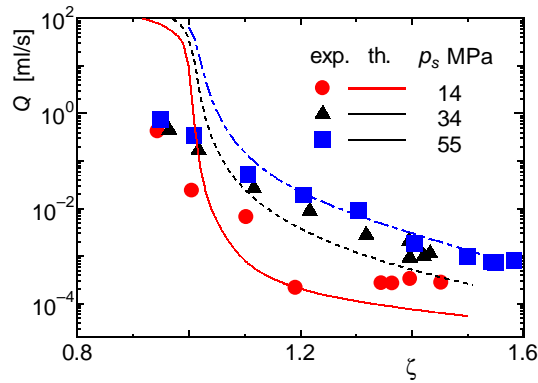


Figure 11. Comparison of leakage flow rate  $Q$  between experiment and theory in consideration of elastic deformation (SUJ2, Smooth).

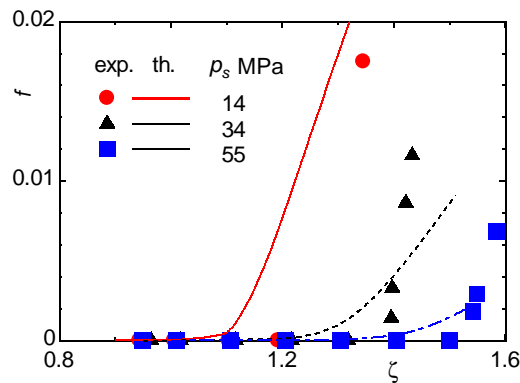


Figure 12. Comparison of equivalent frictional coefficient  $f$  between experiment and theory in consideration of elastic deformation (SUJ2, Smooth).

## 5. Concluding remarks

The experimental work on the hydrostatic thrust bearings in a wide range varying from mixed to fluid film lubrication was carried out under the high pressure and load conditions, using metallic and plastic specimens. The influence of elastic deformation on the bearing characteristics and the optimum conditions was examined experimentally and theoretically. The experimental data indicated that the frictional coefficient increased at a larger hydrostatic balance ratio and the ratio where the power loss minimized exceeded unity when the supply pressure was higher or the bearings consisted of plastics. As the roughness was smaller, the elastic effects also became noticeable.

In parallel, the theoretical study by use of the mixed lubrication model considering elasticity of the bearing parts was conducted. The lubrication model based on the GW model and the PC model, including the elastic deformation as well as adsorbed films, was derived and was solved numerically under the experimental conditions. The theoretical solutions suggested that as the supply pressure increased and/or the elastic modulus decreased, the sealing land of the bearings deformed as a concave shape. The deformation resulted in an increase in the fluid pressure and the hydrostatic load-carrying capacity. As a result, the deformation led to the fact that the hydrostatic balance ratio where the power loss minimized exceeded unity for elastic bearings, whereas the ratio almost equaled unity for rigid bearings. The calculated results based on the present model helped explaining the mechanism and showed a good agreement with the experimental data.

## Acknowledgements

The authors would like to express their thanks to Dr. X. Wang of Yokohama National University and Messrs. T. Yoshida and K. Kitamura of the students of Muroran Institute of Technology for their help on carrying out the experiment and Dr. Jurandir I. Yanagihara of Escola Polit cnica da Universidade de S o Paulo for reading the manuscript.

## References

- Castelli, V., Rightmire, G. K. and Fuller, D. D., 1967, "On the Analytical and Experimental Investigation of a Hydrostatic Axisymmetric Compliant-Surface Thrust Bearing", *Journal of Lubrication Technology, Transactions of ASME*, Vol. 89, pp. 510-520.
- Christensen, H., 1970, "Elastohydrodynamic Theory of Spherical Bodies in Normal Approach", *Journal of Lubrication Technology, Transactions of ASME*, Vol. 92, pp. 145-154.
- Dowson, D. and Taylor, C. M., 1967, "Elastohydrostatic Lubrication of Circular Plate Thrust Bearings", *Journal of Lubrication Technology, Transactions of ASME*, Vol. 89, pp. 237-244.
- Fuller, D. D., 1984, "Theory and Practice of Lubrication for Engineers", 2nd ed., John Wiley & Sons, Inc.
- Greenwood, J. A. and Williamson, J. B. P., 1966, "Contact of Nominally Flat Surfaces", *Proceedings of Royal Society, London, Series A*, Vol. 295, pp. 300-319.
- Hamrock, B. J., 1994, "Fundamentals of Fluid Film Lubrication", International Edition, McGraw-Hill.
- Hibi, A., Ichikawa, T. and Miyagawa, S., 1971, "Flow Characteristics of Cylindrical Chokes (in Japanese)", *Journal of Japan Hydraulics and Pneumatics Society*, Vol. 2, No. 2, pp. 72-80.
- Hooke, C. J. and Li, K. Y., 1988, "The Lubrication of Overclamped Slippers in Axial Piston Pumps--Centrally Loaded Behaviour", *Journal of Mechanical Engineering Science, Proceedings of IMechE*, Vol. 202, No. C4, pp. 287-293.
- Iboshi, N. and Yamaguchi, A., 1982, "Characteristics of a Slipper Bearing for Swash Plate Type Axial Piston Pumps and Motors (1st Report, Theoretical Analysis)", *Bulletin of JSME*, Vol. 25, No. 210, pp. 1921-1930.
- Inazaki, I. and Aoyama, T., 1990, "Hydrostatic Bearing (in Japanese)", pp. 83-123, Kogyo Chosakai.
- JAST (Japanese Society of Tribologists), 2001, "Tribology Handbook (in Japanese)", pp. 83-92, Yokendo.
- Kazama, T., Iwasaki, N. and Yamaguchi, A., 1998, "Effect of Elastic Deformation on Hydrostatic Thrust Bearings for Hydraulic Equipment", *Power Transmission and Motion Control*, pp. 259-268, Professional Engineering Publishing.
- Kazama, T. and Yamaguchi, A., 1993, "Application of a Mixed Lubrication Model for Hydrostatic Thrust Bearings of Hydraulic Equipment", *Journal of Tribology, Transactions of ASME*, Vol. 115, pp. 686-691.
- Kazama, T. and Yamaguchi, A., 1995a, "Experiment on Mixed Lubrication of Hydrostatic Thrust Bearings for Hydraulic Equipment", *Journal of Tribology, Transactions of ASME*, Vol. 117, pp. 399-402.
- Kazama, T. and Yamaguchi, A., 1995b, "Effects of Elastic Deformation on Optimum Design Criteria of Hydrostatic Thrust Bearings for Hydraulic Equipment in Mixed Lubrication", *Proceedings of International Tribology Conference, Yokohama*, pp. 1291-1296, Japanese Society of Tribologists.
- Kazama, T. and Yamaguchi, A., 1997, "Shock Absorption by Oil Films Applicable to Bearing and Seal Parts of Hydraulic Equipment", *Tribology for Energy Conservation*, pp. 195-204, Elsevier.
- Kazama, T., Yamaguchi, A., Wang, X. and Akasaka, Y., 1996, "Experiment on Hydrostatic Thrust Bearings in Mixed Lubrication for High Pressure Hydraulic Pumps and Motors", *Fluid Power*, pp. 431-436, Japan Hydraulics and Pneumatics Society.
- Masuko, M. and Nakahara, T., 1972, "A Basic Study of Hydrostatic Guide Way (2nd Report) (in Japanese)", *Transactions of JSME*, Vol. 38, No. 316, pp. 3235-3245.
- O'Donoghue, J. P. and Rowe, W. B., 1969, "Externally Pressurized Bearing Design Procedures Developed at Lanchester College of Technology", *Proceedings of 10th International M.T.D.R. Conference, Advances in Machine Tool Design and Research*, pp. 409-423, Pergamon Press.
- Patir, N. and Cheng, H. S., 1978, "An Average Flow Model for Determining Effects of Three-Dimensional Roughness on Partial Hydrodynamic Lubrication", *Journal of Lubrication Technology, Transactions of ASME*, Vol. 100, pp. 12-17.
- Patir, N. and Cheng, H. S., 1979, "Application of Average Flow Model to Lubrication between Rough Sliding Surfaces", *Journal of Lubrication Technology, Transactions of ASME*, Vol. 101, pp. 220-230.
- Prabhu, T. J. and Ganesan, N., 1983a, "Non-Parallel Operation of Conical Hydrostatic Thrust Bearing", *Wear*, Vol. 86, pp. 29-41.
- Prabhu, T. J. and Ganesan, N., 1983b, "Eccentric Operation of Conical Hydrostatic Thrust Bearing", *Wear*, Vol. 87, pp. 273-285.
- Rohs, H. G., 1970, "Die Hydrostatische Bewegungspaarung im Werkzeugmaschinenbau", *Konstruktion*, Vol. 22, pp. 321-329.
- Shute, N. A. and Turnbull, D. E., 1963, "Minimum Power Loss of Hydrostatic Slipper Bearings for Axial Piston Machines", *Proceedings of Lubrication and Wear Convention*, pp. 3-14.
- Wang, X. and Yamaguchi, A., 2002a, "Characteristics of Hydrostatic Bearing/Seal Parts for Water Hydraulic Pumps and Motors. Part 1: Experiment and Theory", *Tribology International*, Vol. 35, No. 7, pp. 425-433.
- Wang, X. and Yamaguchi, A., 2002b, "Characteristics of Hydrostatic Bearing/Seal Parts for Water Hydraulic Pumps and Motors. Part 2: On Eccentric Loading and Power Losses", *Tribology International*, Vol. 35, No. 7, pp. 435-442.
- Wilcock, D. F. and Booser, E. R., 1957, "Bearing Design and Application Engineering", pp. 345-366, McGraw-Hill.
- Williams, J. A., 1994, "Engineering Tribology", Oxford Science Publications.
- Yamaguchi, A., 1978, "Tap Water--Possibility as a Hydraulic Fluid (in Japanese)", *Journal of Japan Hydraulics and Pneumatics Society*, Vol. 9, No. 4, pp. 205-210.
- Yamaguchi, A., 1986, "Lubrication in Oil-Hydraulic Equipment (in Japanese)", *Journal of Japan Society of Lubrication Engineers*, Vol. 31, No. 10, pp. 685-690.

- Yamaguchi, A., 1987, "Formation of a Fluid Film between a Valve Plate and a Cylinder Block of Piston Pumps and Motors (2nd Report, A Valve Plate with Hydrostatic Pads)", *JSME International Journal*, Vol. 30, No. 259, pp. 87-92.
- Yamaguchi, A. and Matsuoka, H., 1992, "A Mixed Lubrication Model Applicable to Bearing/Seal Parts of Hydraulic Equipment", *Journal of Tribology, Transactions of ASME*, Vol. 114, pp. 116-121.